LM-02K104
October 11, 2002

Spatial Differencing and Mesh Sensitivity in Two- and Three-Dimensional Discrete Ordinates Codes

C.S. Davidson, C.A. Burre

02-K-104 fi

Nuclear Mathematical and Computational Sciences: A Century in Review, A Century Anew
Gatlinburg, Tennessee, April 6-11, 2003, on CD-ROM, American Nuclear Society, LaGrange Park, IL (2003)

SPATIAL DIFFERENCING AND MESH SENSITIVITY IN TWO- AND THREE-DIMENSIONAL DISCRETE ORDINATES CODES

Chal S. Davidson and Charles A. Burre
Lockheed Martin Corporation
Schenectady, New York

ABSTRACT

Errors due to spatial differencing methods and mesh size in two-dimensional and three-dimensional discrete ordinate solutions of a typical gamma ray shielding problem are illustrated by comparing results from the DORT, TORT, and PARTISN codes. Using a model geometry that is typical of spent fuel transfer and storage casks these errors were systematically investigated by varying the mesh size and differencing method. The results of this study show that the fixed-weighted and adaptive weighted diamond differencing methods in 2D problems require mesh intervals of about 0.25 mfp's for reasonable accuracy in deep penetration. The number of mesh cells required for weighted diamond difference methods severely limit the size of 3D problems that can be solved. The linear discontinuous method in PARTISN is shown to maintain numerical accuracy in 3D problems while reducing the overall computational effort by allowing larger mesh intervals. It is also shown that 3D problems exhibit differencing errors that may not readily be inferred from 2D results. Comprehensive displays of the magnitudes of spatial differencing errors in a practical shielding problem provide valuable guidance for the shielding practitioner using today's computational tools.

Key Words: adaptive weighted diamond differencing, linear discontinuous, linear nodal

1. INTRODUCTION

Discrete ordinate codes, such as DORT, TORT (Reference 1), and PARTISN (Reference 2), obtain solutions to the transport equation by iteratively solving a finite difference approximation for the spatial variation of the directional particle flux in each of the spatial mesh cells of the problem. Spatial differencing methods have evolved from their initial appearance in production codes as the constraints of accuracy, stability, computational efficiency, and problem scope have played out, References 3-7. A subset of those methods that are still in general use in current two-dimensional (2D) and three-dimensional (3D) applications includes the fixed weighted diamond difference (FW), adaptive weighted diamond difference (AWDD), theta weighted diamond difference (TW), linear discontinuous (LD), linear nodal (LN), and linear characteristic (LC) methods. References 4-7 provide the motivation, mathematical derivations, and error evaluations for several of these methods.

The original diamond difference method (DD), which assumes a linear relationship between the directional flux at the cell center and cell boundaries, is simple and accurate for small mesh intervals. When the mesh interval is too large, as measured along the discrete direction through the cell, the difference equations yield negative fluxes on one or more faces of the cell. These negative directional fluxes cause oscillations in the iterative process and the spatial flux solution and can frequently cause the scalar flux to be negative. To overcome this, the FW, AWDD, and

TW variations on the DD method were developed to minimize or eliminate the appearance of negative fluxes without significantly sacrificing computational cost or accuracy. To be sufficiently accurate, these methods require a fairly fine spatial mesh, which can readily be achieved for 2D problems on current computer platforms.

The accuracy and stability of these methods as a function of mesh spacing is illustrated for a realistic gamma ray shielding problem. Gamma-ray shielding problems require smaller physical mesh intervals than neutron shielding problems because the mean free path (mfp) length is smaller (for example, for fast neutrons in water the mfp is 10 cm versus about 2 cm for the gamma rays of interest from spent fuel). Extensive results of mesh sensitivity in 2D are given to indicate the practical limitations of these methods and to set the stage for 3D sensitivities.

The LN and LC methods improve on the weighted DD methods by employing a higher order approximation to the spatial variation throughout the cell. The LD method still assumes linear variation across the cell but achieves greater accuracy by allowing the directional fluxes to be piecewise continuous across the cell boundaries. These methods are, of course, computationally more expensive, but their greater accuracy allows for coarser mesh intervals, which can offset the cost in 3D. The solution from three such methods, TORT's LN and LC methods and PARTISN's LD method are compared in this study to illustrate their performance in realistic 3D shielding problems.

2. DESCRIPTION OF MODEL PROBLEM

The model for these studies is a hypothetical fuel bundle and spent fuel handling cask composed entirely of iron and air. The geometric arrangement, shown in Figure 1, consists of a cylindrical source region, 40 cm in length with a 10 cm radius, that is separated from an identical iron cylinder by a 20 cm region of air. This arrangement is encased in a 0.5 cm iron shell and surrounded by a 9.5 cm air gap that allows modeling of axial streaming, as would be seen around the fuel rods in a typical storage cask. The cask itself is modeled by a 40 cm thick cylindrical iron shell (similar to the model used in Reference 8) with a 10 cm bottom cap and a 10 cm lip at the top. The entire cask has a radius of 60 cm, a height of 140 cm, and is surrounded on the sides and top by a 10 cm thick blanket of air. Although not shown in Figure 1, the outer air region is a rectangular prism in XYZ geometry. This problem was modeled exactly in 2D RZ geometry and was approximated by 'staircase' material boundaries on a uniform mesh in XYZ geometry in the 3D studies.

The energy distribution of the gamma ray source was modeled from a ^{134}Cs decay spectrum. This is an important source in spent fuel after a few years decay, Reference 9. The energy group structure that was used contained 14 groups from 0.001 to 1.4 MeV. The highest ^{134}Cs source energy is 1.365 MeV. The gamma ray cross sections were processed from the PHOTB6 library (Reference 10) with NJOY99.50 (Reference 11) and TRANSX2.15 (Reference 12). The Legendre expansion of the scattering cross sections was limited to P_3 to allow more memory for spatial mesh refinements. A higher order may be necessary for accuracy in deep penetration problems. It is also noted that some of the negative fluxes discussed below are the result of the low expansion order. The group fluxes from each solution were converted to an air kerma response and summed over all energy groups.

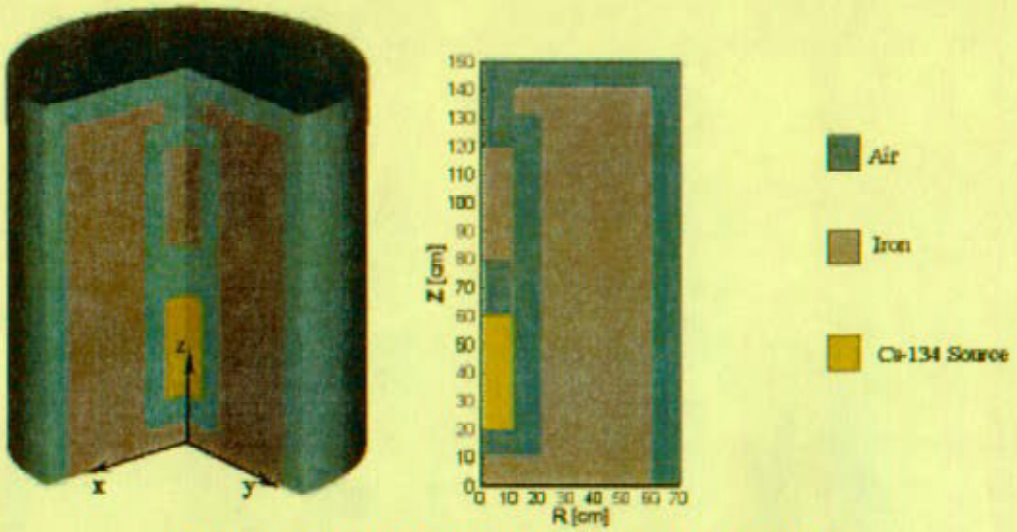

Figure 1. Iron cask problem geometry in 3D and 2D.

For the 2D studies, a special Z-biased quadrature was used that contained 135 angles per octant distributed on 20 cones about the z-axis. Quadratures of this type are sometimes needed to accurately treat axial streaming in the annular air gaps. It is recognized that such a quadrature will provide a severe test of spatial differencing methods because many of the angles will be almost parallel to the vertical faces of the cell. In the 3D studies the quadrature was reduced to the standard S16 set (36 angles per octant) to reduce running time requirements.

3. SENSITIVITY STUDIES IN 2D MODELS

3.1. Description of Cases Studied

Three variations of the weighted diamond method were studied in 2D RZ models. One group of studies investigated the mesh sensitivity of DORT TW solutions. Several other groups of studies investigated the mesh sensitivity of the FW[1] and AWDD methods in PARTISN solutions. The choice of FW or AWDD in PARTISN is specified by the *wdamp* parameter. If a *wdamp* value of less than 1.0 is input, a fixed weight, equal to *wdamp,* is used in the FW diamond difference method. When *wdamp* is greater than or equal to 1.0, the AWDD is used. Reference 7 demonstrated that values of the fixed weight should be between 0.5 and 0.6 to achieve accuracy and stability. For DORT the standard set-to-zero negative flux fixup method was specified while no negative fixup was used in PARTISN. The DORT runs were made with mesh intervals (Δ) of 0.25, 0.5, 0.75, and 1 cm. The PARTISN runs were made with mesh intervals of 0.25, 0.5, and 1 cm. The FW runs were made with *wdamp* values of 0.53, 0.55, and 0.6 and the AWDD runs used a *wdamp* value of 1.0.

[1] The FW method was added to a local version of PARTISN by the Bechtel Corp.

3.2. Comparison of Results

After evaluating the solutions from each run and plotting the ratios of various cases, it was evident that the solutions converged to similar values over most of the solution space as the spatial mesh interval was refined. The FW run using *wdamp*=0.55 and Δ=0.25 cm was chosen as the base case for three reasons. First, there was minimal change between the Δ=0.25 cm and Δ=0.5 cm solutions, for deep penetration in the radial direction, indicating good spatial convergence. Second, the choice of *wdamp* equal to 0.55 along with the small mesh size provided a solution that minimized the appearance of negative fluxes without employing any type of fixup. Third, the solution converged smoothly with no oscillatory behavior from one iteration to the next.

In order to show the change in the solution at any point relative to the base case, the response from each solution was divided by that of the base case. Point-by-point ratios of cases with different spatial mesh were formed by first mapping the finer mesh case onto the coarse mesh grid using linear interpolation on the log of the response. Figure 2 displays the spatial convergence of each case compared to the base case at the location r=50 cm and z=40 cm. This is a well-behaved region representing deep penetration at the axial midplane of the source. As the spatial mesh is refined, all solutions converge towards the base case. The AWDD, TW, and FW (*wdamp*=0.53) solutions approach the converged result from below while the FW (*wdamp*=0.6) solution approaches from above. The ratio of any given case to the converged solution represents the compounded error associated with the approximation of exponential attenuation by a linear extrapolation through the mesh cells. The TW and AWDD solutions for Δ=0.25 cm would also have been reasonable choices for the converged solution at the point shown in Figure 2. However, they were not selected because they underestimated the converged value at Δ=1 cm by a larger amount than the chosen base case.

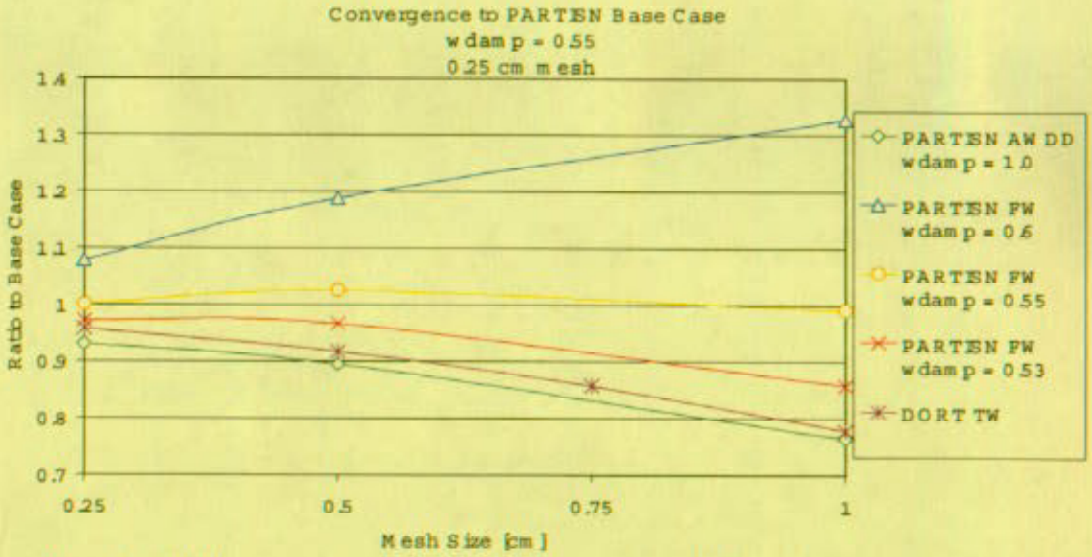

Figure 2. Solution convergence with mesh refinement for point located at r=50 cm, z=40 cm.

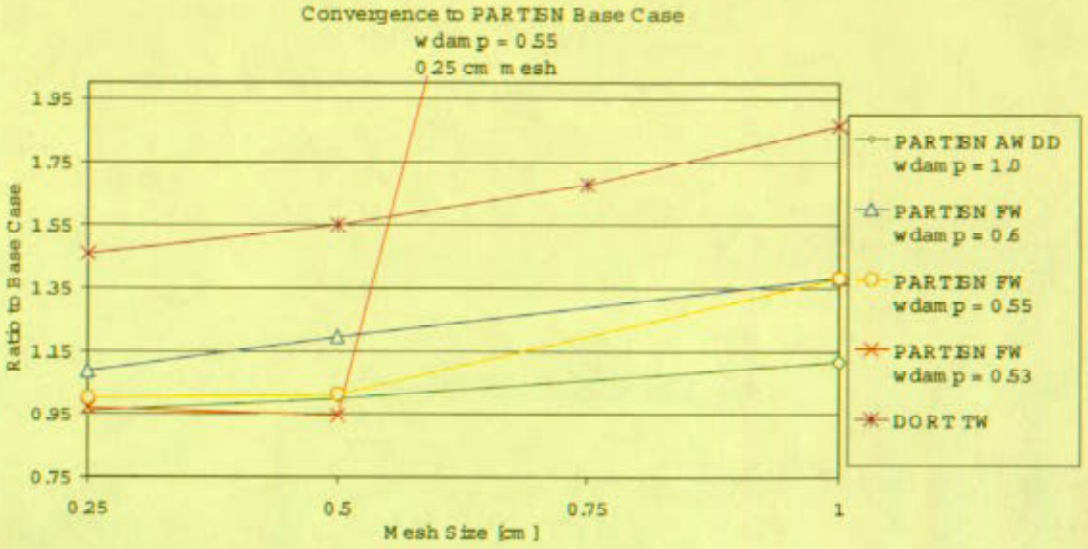

Figure 3. Solution convergence with mesh refinement for point located at r=40 cm, z=120 cm.

Figure 3 shows the spatial convergence trends at the location r=40 cm and z=120 cm. This is a problematic region, in which negative fluxes appear for the larger mesh intervals in the FW (*wdamp* = 0.53 and *wdamp* = 0.55) cases and in which the AWDD and TW methods give different results. It appears that all of the PARTISN solutions are converging to the same value while the DORT solution is converging to a higher value. These effects will be discussed in more detail below. At this point the AWDD solution appears to be the most stable for the larger mesh sizes.

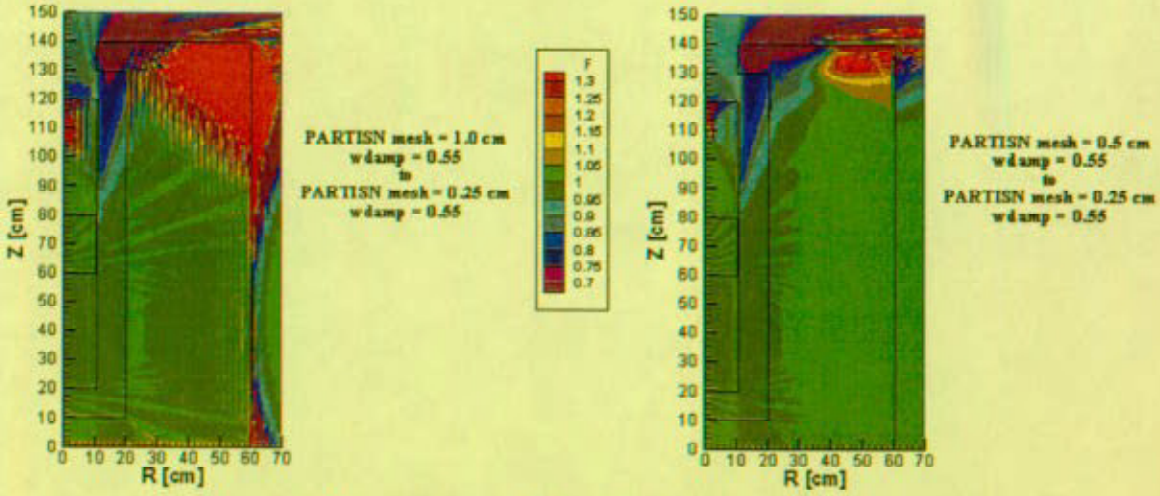

Figure 4. Mesh sensitivity in PARTISN FW (wdamp=0.55) solutions.

Figure 4 shows the mesh sensitivity in the FW (*wdamp*=0.55) solutions. For deep penetration radially outward, the Δ=0.5 cm solution (on the right) shows a gradual increase reaching 4% at the outside of the cask relative to the base case. The Δ=1.0 cm solution (on the left) appears even closer to the base case, but is hampered by sharp point-to-point oscillations, which are discussed below. The convergence trend in Figure 2 also shows that the FW (*wdamp*=0.55) solution is actually closer to the base case at Δ=1.0 cm than at Δ=0.5 cm due to an overshoot of the Δ=0.5 cm solution.

Figure 5 shows the locations of negative total response calculated with the FW method with *wdamp*=0.53 and 0.55. These locations clearly correlate with the oscillations and areas of large differences seen in Figure 4 and other similar plots. This oscillatory behavior can also lead to a divergent source iteration process. The prevalence of negative fluxes can be reduced by increasing *wdamp* to 0.6 or by making the mesh intervals smaller. The AWDD method eliminated all negative fluxes except for the small pocket on the z-axis at z=110 cm. The negative flux in this area is caused by negative backscattering from the inner bore of the cask due to the P_3 expansion. DORT's negative fixup eliminates the negative scattering sources.

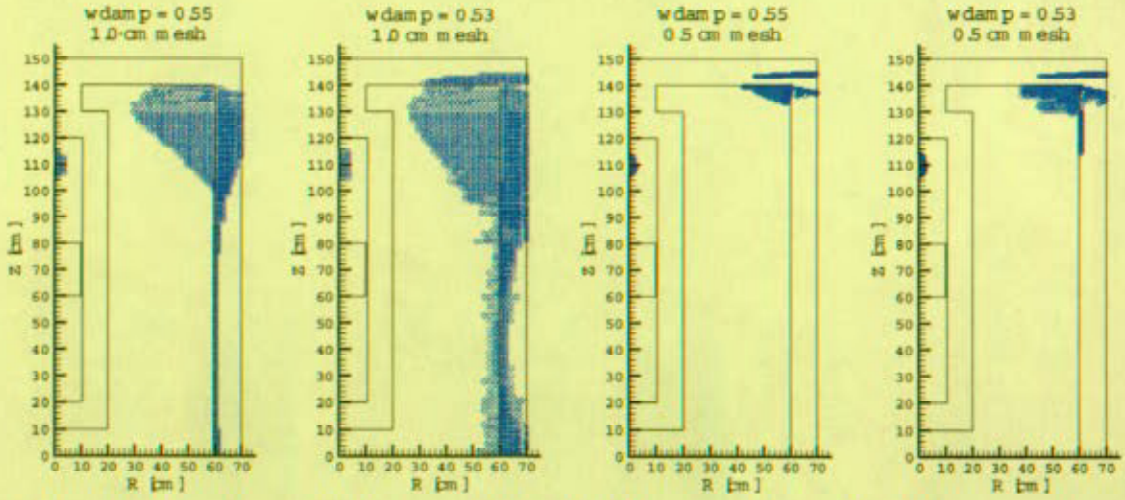

Figure 5. Change in negative flux concentration for different mesh sizes and weighting parameters.

Ratios of the AWDD solutions for Δ=1 cm and Δ=0.5 cm to the base case are given in Figure 6. For Δ=0.5 cm, the solution is within 10% of the base case for r<50 cm and z<110 cm. For Δ=1 cm, the solution is more than 10% lower than the base case at the source elevation for r>30 cm and is more than 25% lower at the outside of the cask. At the higher elevations, the AWDD solutions agree well with the base case except in the problematic region near the outer corner of the cask, where the AWDD solution is 30% or more higher than the base case.

Ratios of the DORT TW solutions to the base case are given in Figure 7. At the source elevation, the solutions are very similar to the AWDD solutions due to the similarities in the methods when there is no tendency toward negative fluxes. Above z=110 cm, DORT is 40%, or more, higher

than the base case throughout the thickness of the cask. This is probably due to the combined effects of DORT's fixup of the negative scattering sources and the theta-weighted differencing.

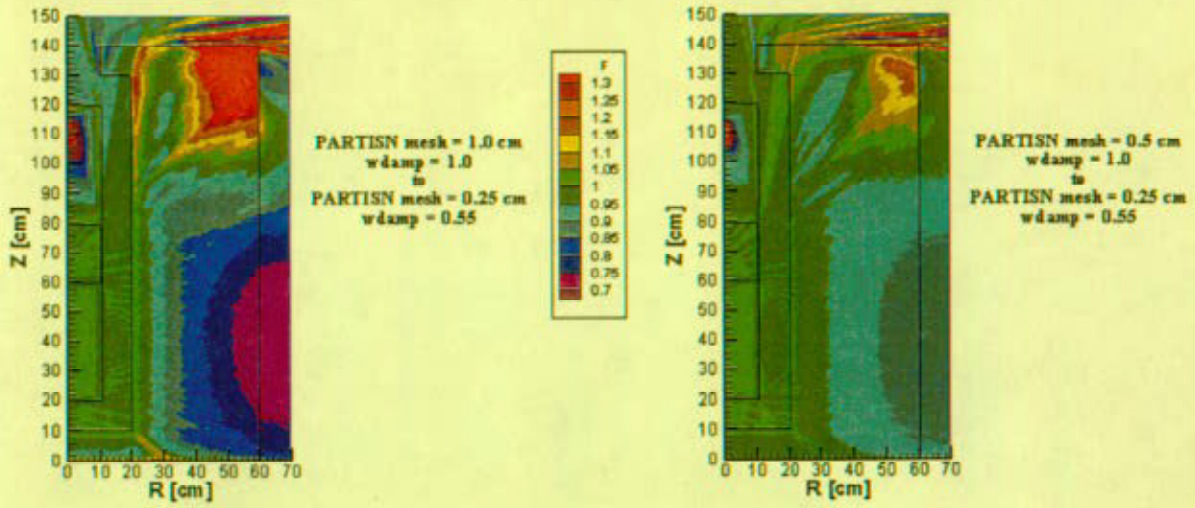

Figure 6. Ratio of PARTISN AWDD solutions for 1.0 and 0.5 cm mesh intervals to base case.

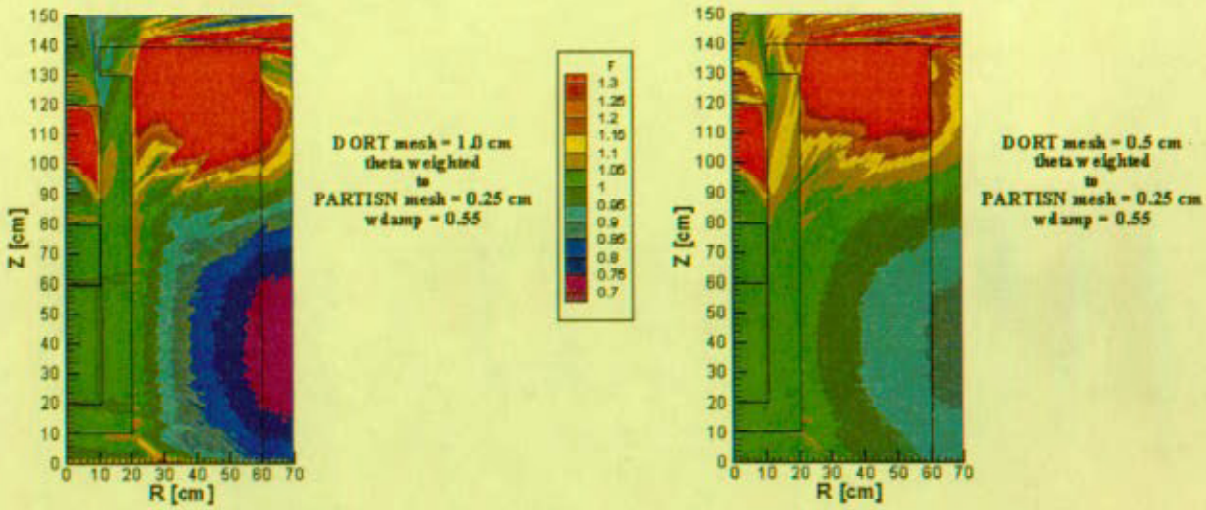

Figure 7. Ratio of DORT TW solutions for 1.0 and 0.5 cm mesh intervals to base case.

3.3. Conclusions from 2D Sensitivity Studies

For a mesh interval of 0.5 cm (approximately 0.25 mfp), the FW (*wdamp*=0.55), TW, and AWDD methods provide solutions that are converged to within 10% over most of the solution space. The DORT TW results are significantly higher than the other methods in problematic regions (regions where DD methods produce negative fluxes). For larger mesh intervals, oscillatory behavior and negative fluxes may result for FW methods and the errors with TW and

AWDD will exceed 10% in both the positive and negative directions. Higher order differencing methods would probably produce acceptable results for larger mesh sizes, however, these methods are generally not employed in 2D. Realistic problems can be solved with mesh intervals of the order of 0.25 mfp's on readily available computers even if an increase in angular quadrature, energy groups, or scattering order, were required.

4. SENSITIVITY STUDIES WITH 3D MODELS

4.1. Description of Cases Studied

The effects of spatial differencing and mesh sensitivity in the TORT and PARTISN codes were investigated for 3D XYZ models of the problem described above. For uniform mesh intervals of 1, 0.5, and 0.25 cm, the problem requires 0.756×10^6 cells[2], 5.88×10^6 cells, and 47×10^6 cells, respectively. The Δ=0.25 cm case was prohibitively expensive to run, so only comparisons of the Δ=0.5 cm and Δ=1 cm solutions are given. Studies were performed using the FW, AWDD, and LD methods in PARTISN and the LN and LC methods in TORT. For the FW cases only the *wdamp*=0.55 and 0.6 cases were run because severe negative flux and stability issues were expected with *wdamp*=0.53.

4.2. Comparison of Results

Identification of a spatially converged result for the 3D cases was more difficult than for the 2D cases, not only because the Δ=0.25 cm results were not available, but also because all methods showed substantially different solutions in the upper third of the cask for the two mesh intervals studied. However, for the Δ=0.5 cm cases, the LN, LC, LD, and FW(*wdamp*=0.55) results all agreed to within about 15% for all points below z=100 cm. This is the region of greatest practical significance, where direct penetration through the shield would set the design thickness of the cask. The general agreement of these methods provides a strong indication that each of the solutions are near the spatially converged result. As will be discussed below, the AWDD and the FW (*wdamp*=0.6) solutions for Δ=0.5 cm exhibited larger differences in these regions.

At the higher elevations (z>120 cm), TORT's LN and LC solutions were very close to each other but higher than the LD solution by more than 75%. PARTISN's LD solution was the least sensitive to doubling the mesh spacing in this area and it agreed with the FW (*wdamp*=0.55) solution for Δ=0.5 cm. Therefore, the LD solution was chosen to be the base case for displaying the relative differences among the solutions. It is recognized that this is a somewhat arbitrary selection and that further analysis is needed to establish a spatially converged result in the problematic region. The various 3D solutions are compared to the base case in Figures 8 to 11. These Figures show the ratio of the solutions to the base case on the planes at x=0, y=0, z=40, and z=120 cm.

[2] Since one of the material boundaries is at 10.5 cm, one additional mesh interval was needed in the x and y directions.

The change in the LD solutions between the Δ=1 cm and Δ=0.5 cm cases is shown in Figure 8. The solution increases by less than 15% over 80% of the model when the mesh spacing is increased to 1 cm, or approximately 0.5 mfp. Some of the solution differences near the inner wall of the cask (r=20 cm) could be due to the stepping of the materials in the Cartesian mesh cells to approximate the cylindrical surfaces. This causes a real difference in the material boundaries of the two differently meshed problems. These differences are most apparent in the z=120 plane. However, the good agreement between the solutions throughout the thickness of the cask indicates that these differences only affect localized areas near the cylindrical boundaries.

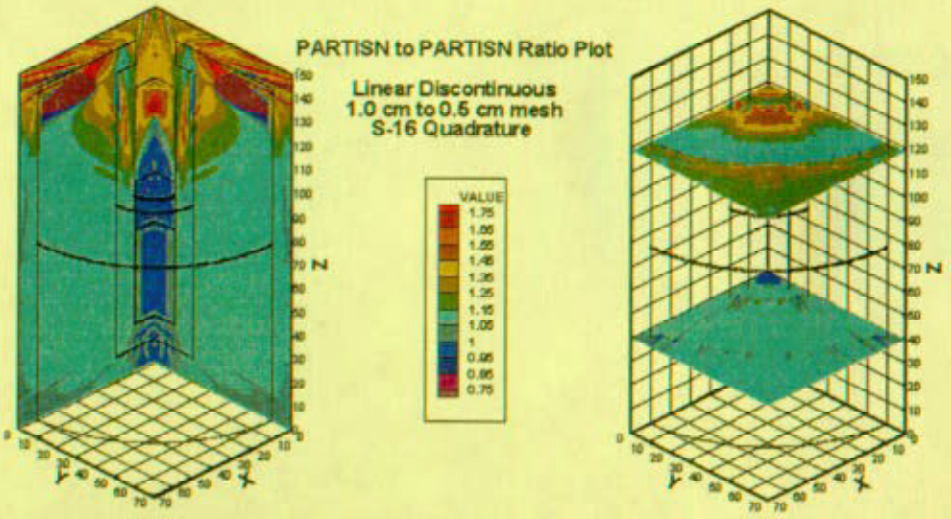

Figure 8. Mesh sensitivity in PARTISN LD solutions (Ratio of solutions for 1.0 cm to 0.5 cm mesh).

The FW (*wdamp*=0.55, Δ=0.5 cm) solution is compared to the base case in Figure 9. The FW solution is slightly higher, by up to 15%, throughout virtually the entire cask for z<125 cm. Based on the spatial convergence of the FW solutions in 2D, it is expected that an FW solution with somewhat smaller mesh spacing would agree more closely with the LD solution. The LD method in PARTISN takes about three times longer per mesh cell per iteration than the FW method. Since the LD solution for Δ=1 cm, which has one-eighth the number of cells, is approximately equivalent to the FW solution for Δ=0.5 cm, the computing cost of the LD solution is approximately 38% of the cost of an equivalent FW solution.

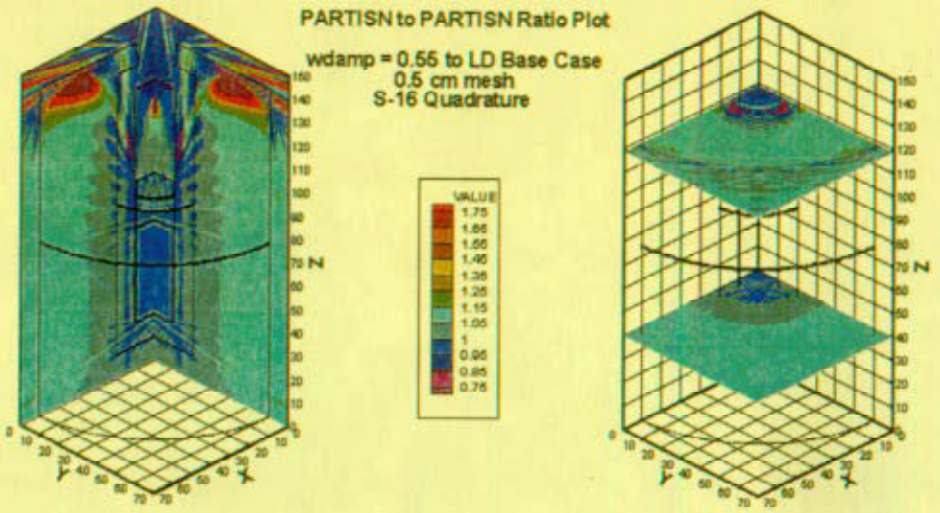

Figure 9. Ratio of PARTISN FW (*wdamp*=0.55) and LD solutions for a 0.5 cm mesh interval.

The differences between the FW (*wdamp*=0.6) solution and the base case in 3D were similar to, but somewhat larger than, the differences observed in the 2D models. The FW solution was higher than the base case by about 35% at the outside of the cask for Δ=0.5 cm and by 75% for Δ=1 cm.

The LN solution from TORT (*mode*=2) is compared to the LD solution from PARTISN for Δ=0.5 cm in Figure 10. While agreeing very well (within 5%) at the elevation of the source, the LN solution becomes progressively higher with elevation. The difference is 15% at z=110 cm and rapidly increases to more than 75% at higher elevations. Although not shown, the LC solution was virtually identical to the LN solution. The reason for the higher solutions with TORT LN and LC has not been investigated, but could be due to measures built into the TORT methods to insure positive fluxes, Reference 6. Moreover, the difference between the LN (or the LC) solutions for Δ=1 cm and Δ=0.5 cm on the z=120 plane was larger than for the LD method. The solution ratios for the LD cases at z=120 cm, Figure 8, indicate a large area in the outer half of the cask where the solution changed by less than 15% with the mesh refinement. With the LN cases, the solution changed by 15 to 35% over the same area. Although the effects of the different material boundaries in the Δ=1 cm and Δ=0.5 cm cases cloud this comparison, it appears that the LD method has less sensitivity to mesh spacing in this area. These results are not unlike the mesh sensitivities reported for the LD and CLN/F (constant linear nodal method with negative flux fixup) methods, Reference 13.

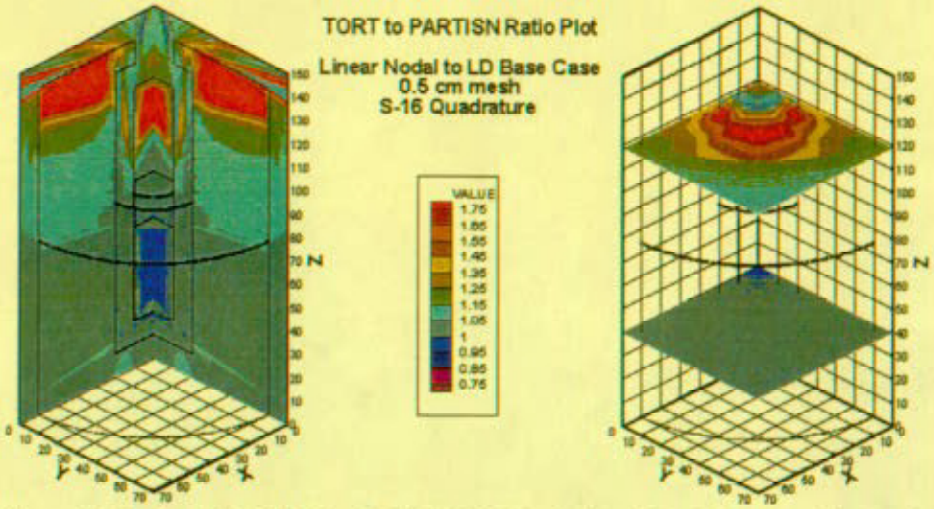

Figure 10. Ratio of TORT LN and PARTISN LD solutions for a 0.5 cm mesh interval.

In the 2D studies it was observed that the AWDD solution agreed well with the spatially converged FW solutions. In the comparison of the 3D AWDD and LD solutions, shown in Figure 11, it is noted that the ratios on the x=0 and y=0 planes are similar to the ratios from the 2D studies, in which AWDD solution was about 10% below the base case at the outside of the cask. However, the ratios in the z=40 plane show a significant departure from the expected azimuthal symmetry at the midplane of the source. Along the 45° diagonal to the x and y-planes at the source elevation, the AWDD solution is up to 40% larger than the LD solution. The magnitude of the difference is larger for Δ=1 cm. Although TORT's TW method was not tried in these studies, a similar phenomena was observed in mesh sensitivity studies for neutron problems. The asymmetric azimuthal distributions were not observed in the FW (*wdamp*=0.55), LN, and LC solution ratios. This indicates that the sensitivities that can arise in 3D models may not be readily inferred from 2D model results.

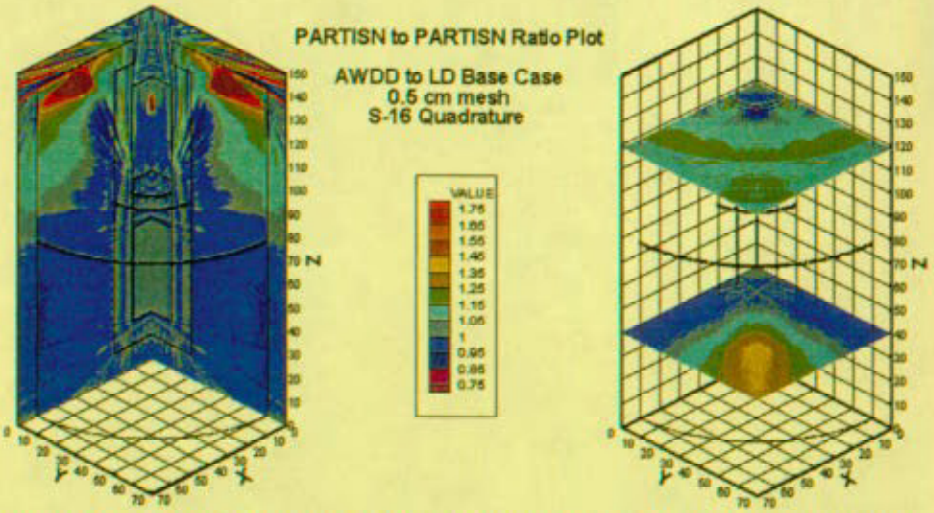

Figure 11. Ratio of PARTISN AWDD and LD solutions for a 0.5 cm mesh interval.

4.3. Conclusions from 3D Sensitivity Studies

For a mesh spacing of 0.5 cm (about 0.25 mfp), the LN, LC, LD, FW (*wdamp*=0.55) methods gave solutions that agreed among each other to within 15% over most of the model fuel cask below z=110 cm. When the mesh spacing was doubled, the LD solution changed by the smallest amount. The FW (*wdamp*=0.55) was unstable at Δ=1 cm, while the FW solution with *wdamp*=0.6 appeared to have poor accuracy for both mesh intervals. The AWDD (*wdamp*=1.0) solution exhibited anomalous behavior along the 45° diagonal between the x and y planes at the source elevation. Therefore, of the methods studied here, the LD method in PARTISN seems to offer the most accurate solution for a 3D gamma-ray shielding problem.

The accuracy of LD method for a Δ=1 cm mesh (about 0.5 mfp) was comparable to that of the FW solution for Δ=0.5 cm. The LD method requires three times as much computational work as the FW method, but this is more than offset by the factor of eight reduction in the number of mesh cells in this case. Therefore, as long as larger mesh spacing can be tolerated from a material boundary standpoint, the LD method will require less computer resources.

These conclusions are specific to the particular problem studied here. It is acknowledged that spatial convergence in the 3D cases was not fully demonstrated, nor were the errors due to the other discrete approximations fully separated from the spatial differencing errors. Nevertheless, these results demonstrate the magnitude and distribution of differences that can result when popular methods are applied to practical shielding problems.

ACKNOWLEDGMENTS

Acknowledgement is given to the Los Alamos National Laboratory for providing a developmental version of PARTISN.

REFERENCES

1. W. A. Rhodes and D. B. Simpson, "The TORT Three-Dimensional Discrete Ordinates Neutron/Photon Transport Code," ORNL/TM-13221, October (1997).
2. R. E. Alcouffe and R. S. Baker, "Time-Dependent Deterministic Transport on Parallel Architectures Using PARTISN," *Proc. of the 1998 ANS Radiation Protection and Shielding Topical Conf.*, Nashville, TN, April 19-23, Vol. 1, pp. 335-342 (1998).
3. K. D. Lathrop, "Discrete-Ordinates Method for the Numerical Solution of the Transport Equation," *Reactor Technology*, **15**, pp.107-135 (1972).
4. W. F. Walters, and R. D. O'Dell, "A Comparison of Linear Nodal, Linear Discontinuous, and Diamond Schemes for Solving the Transport Equation in (x,y) Geometry," *Trans. Am. Nuc. Soc.*, **39**, pp. 465-467 (1981).
5. R. E. Alcouffe, "An Adaptive Weighted Diamond-Differencing Method for Three Dimensional *XYZ* Geometry," *Trans. Am. Nuc. Soc.*, **68A**, pp. 206-209 (1993).
6. R. L. Childs and W. A. Rhodes, "Theoretical Basis of the Linear Nodal and the Linear Characteristic Methods in the TORT Computer Code," ORNL/TM-12246, January (1993).

7. N. K. Madsen, "Convergence of the Weighted Diamond Difference Approximations to the Discrete Ordinates Equations," *Proc. 4th Biennial Topical Meeting of the Math. and Comp. Div. of the ANS*, Idaho Falls, ID, March 29-31, Vol. II, pp. 565-576 (1971).
8. A. F. Avery and H. F. Locke, "NEACRP Comparison of Codes for the Radiation Protection Assessment of Transportation Packages: Solutions to Problems 1-4," NEACRP-L-331, March (1992).
9. A. F. Avery and H. F. Locke, "NEACRP Comparison of Codes for the Radiation Protection Assessment of Transportation Packages," *Proc. of 8th International Conference on Radiation Shielding,* Arlington, TX, April 24-28, Vol. 2, pp.731-737 (1994).
10. D. E. Cullen, *et. al.*, UCRL-50400, Vol. 6, Rev. 5 (September 1997), RSICC Distribution Package DLC-179/ENDLIB-97.
11. R. E. MacFarlane and D. W. Muir, "The NJOY Nuclear Data Processing SystemVersion 91," LA-12740-M, October 1994.
12. R. E. MacFarlane, "TRANSX 2: A Code for Interfacing MATXS Cross-Section Libraries to Nuclear Transport Codes," LA-12312-MS, July 1992.
13. T. A. Wareing and R. E. Alcouffe, "An Exponential Discontinuous Scheme for X-Y-Z Geometry Transport Problems", *Proc. of the 1996 Topical Meeting on Radiation Protection and Shielding,* No. Falmouth, MA, April 21-25, Vol. 2, pp. 597-604 (1996).